Journal of Applied Polymer Science

Preparation of cinchonine molecularly imprinted photonic crystal film and its specific recognition and optical responsive properties

Yanan Zhang, Shaomei Huang, Chuntong Qian, Quanzhou Wu, Jianfeng He
School of Chinese Materia Medica, Guangzhou University of Chinese Medicine, Guangzhou 510006, China
Correspondence to: J.-F. He (E-mail: syrinx@gzucm.edu.cn) or Q.-Z. Wu (E-mail: gzywqz@gzucm.edu.cn)

ABSTRACT: The cinchonine molecularly imprinted photonic polymer (MIPP) film was prepared by using methacrylic acid as functional monomer, ethylene glycol dimethacrylate as cross linker, benzoyl peroxide and N,N-dimethylaniline as initiation system by a combination of colloidal crystal template method and molecular imprinting technique. The structure and morphology of the polymer film were characterized by infrared spectra and scanning electronic microscope. The results exhibit that a highly ordered three-dimensionally interconnected macroporous array with typical face-centered cubic (fcc) structure was formed in the MIPP film. The binding experiments showed that the special, hierarchical porous structure enabled this polymer to possess rapid adsorption kinetics, improved binding capacity, and specificity to analytes. The Bragg diffractive measurements showed that the MIPP film has good specific responsiveness for the template molecules. The Bragg diffraction peaks shifted from 527 to 503 nm with the concentration of the cinchonine varying from 0 to 10^{-3} mol/L, whereas there were no obvious peaks shifts for its structural analogues. This may be ascribed that the changes in the lattice constants and the average refractive indices of MIPP film caused by the special adsorption of template molecules toward recognition sites. © 2015 Wiley Periodicals, Inc. J. Appl. Polym. Sci. **2016**, *133*, 43191.

KEYWORDS: adsorption; characterization; copolymers; films; molecular recognition

Received 2 June 2015; accepted 2 November 2015
DOI: 10.1002/app.43191

INTRODUCTION

Molecular imprinting technology creates a prospective approach to design specific recognition sites within a polymer network via the template polymerization process. Owing to the affinity and high selectivity of the molecularly imprinted polymer (MIP), MIP has been widely exploited in solid-phase extraction, chromatographic separation, chemical sensors, drug carrier, etc.[1–5] Generally, the preparation of MIP is based on bulk polymerization, and need grind and sieve to produce irregular particles. This technique is a conceptually simple and straightforward method for a wide variety of target molecules. In order to maintain the shape and mechanical stability of imprinting cavities and retain a permanent memory for imprinting molecules, the structure of the polymers needs to be rigid enough with a highly cross-linked polymer network. However, the polymer still has some disadvantages, such as restricting mobility of the analyte molecules, embedding of most binding sites, and lower binding kinetic due to long diffusion paths in the bulk.[6,7] To solve these problems, some novel imprinting strategies such as surface imprinting,[8] molecular imprinting nanotechnologies,[9] and porous molecularly imprinted polymer preparation have been proposed.[10]

Photonic crystal with highly three-dimensionally ordered interconnected macroporous (3DOM) structure has drawn considerable attention for the development of various chemical and biological sensors.[11–13] Because of their periodic porous structure, such materials exhibit fascinating Bragg diffraction and bright structural colors. Lately, a new molecularly imprinted photonic polymer (MIPP) has been prepared by the combination of colloidal crystal template method and molecular imprinting technique.[14–16] In this technique, the MIPP were commonly prepared by using a closest-packing colloidal crystal as template (Figure 1). A pre-polymerization solution was infused and polymerized in the voids of the colloidal crystal template. After removal of the colloidal crystal template and molecularly imprinted template, the MIP film of the inverse opal structure displays a 3DOM array with a thin polymer wall, in which nanocavities complementary to analytes in shape and binding sites are obtained. Because of 3DOM structure, such MIPP provides more interaction sites, and can also offer increased mass transport and easier accessibility for the analytes to the recognition sites. This material is particularly suitable for imprinting some biomacromolecules, such as proteins, sugar, and nucleic acid. Meanwhile, the change of the periodic lattice spacing of MIPP film can give rise to interesting optical

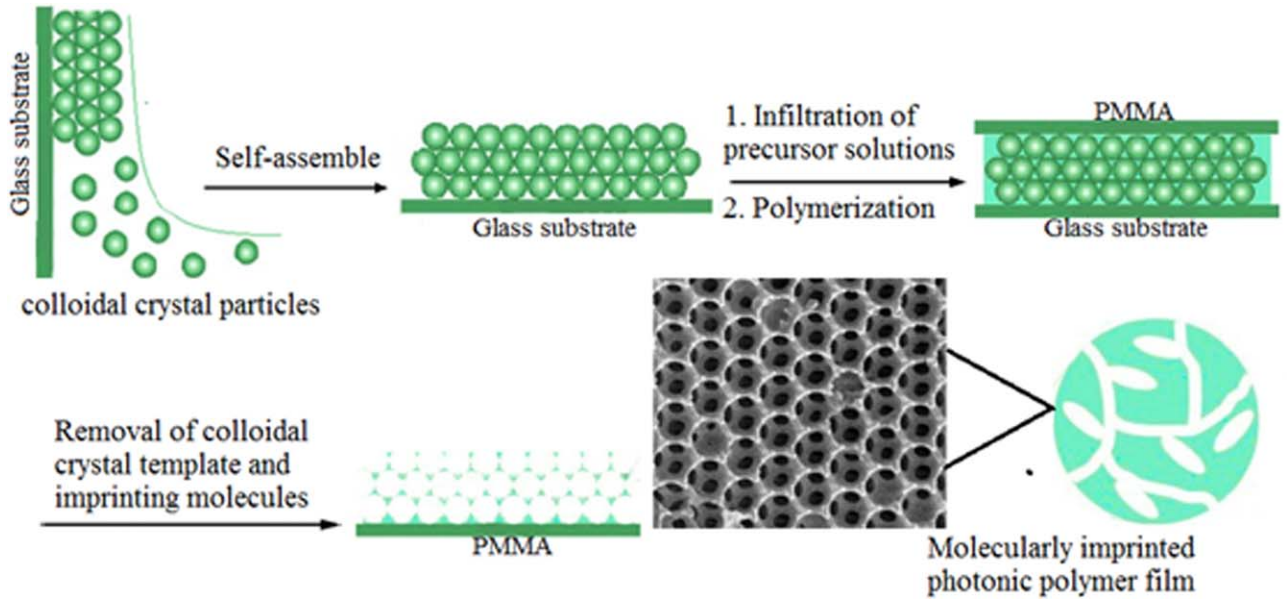

Figure 1. Schematic diagram of the preparation method for MIPP film. [Color figure can be viewed in the online issue, which is available at wileyonlinelibrary.com.]

properties, which can be used to optically determine analytes by means of the shift of Bragg diffraction.[17]

In recent years, MIPP were introduced and then have been further developed by Li's group.[18–20] Presently, MIPP were mostly prepared based on the silica colloidal crystal template, and its application focused on the studies on their sensing properties. Cinchonine, as a cinchona alkaloid, is usually used to treat malaria in medicine. Previous studies have proved cinchonine to be an ideal imprinting molecule. The MIP prepared with cinchonine as template showed pronounced imprinting effect and high selectivity.[21] To further understand the binding characteristics and its optical sensing properties for MIPP material, in this study, the MIPP films were prepared by utilizing polystyrene (PS) as the colloid crystal template and cinchonine as the molecular imprinting template, respectively. The assemblies of the PS colloidal crystal film and the properties of photonic polymer such as adsorption dynamics, binding specificity in contrast to the traditional bulk MIP film were investigated in detail. In addition, the optical responsive properties of the MIPP film toward the template molecules and its structurally similar compound were also evaluated.

EXPERIMENTAL

Materials and Apparatus

Ethylene glycol dimethacrylate (EDMA) and methacrylic acid (MAA) were obtained from Aladdin Chemistry Co. Ltd. (Shanghai, China) and distilled to remove the inhibitor before use. Quinoline was purchased from Jiangsu Yonghua Chemical Reagent Company (Jiangsu, China). Cinchonine and quinine were Acros products. N,N-dimethylaniline was obtained from Tianjin Fuchen Chemical factory (Tianjin, China). Benzoyl peroxide was purchased from Tianjin Damao Chemical Reagent Company (Tianjin, China). Other reagents were all of analytical grade.

All binding experiment and ultraviolet–infrared (UV–vis) spectra were performed using a Tianmei UV-1100 spectrophotometer. Fourier transform infrared (FT-IR) spectrum was recorded on a Vector-22 FT-IR spectrophotometer. The morphology of photonic polymers was observed by a ZSM-6300 field emission scanning electron microscope (FESEM) on gold-sputtered sample. Nitrogen adsorption measurements were performed on a Micromeritics ASAP 2020 apparatus. Surface areas were calculated by the Brunauer–Emmett–Teller (BET) method.

Preparation of Polystyrene Photonic Colloidal Crystal Templates

PS microspheres were synthesized by emulsifier-free emulsion polymerization according to the previous report.[22] The obtained PS colloid particles were dispersed in distilled water or anhydrous ethanol with different concentrations. Common glass slides (25.4 × 76.2 mm) were immersed in a H_2SO_4/H_2O_2 (7 : 3, v/v) mixture for 24 h, followed by rinsing with distilled water and then dried prior to use. Then the treated slides were dipped vertically into the PS solution at 45°C for 24 h. After the solvent was evaporated, the PS colloid crystal films were obtained.

Preparation of Cinchonine MIPP Film

About 0.0147 g of cinchonine (0.05 mmol), 0.0172 g of MAA (0.2 mmol), and 0.0334 g of EDMA (0.16 mmol) were dissolved in 1.0 mL of anhydrous ethanol, and then were stored overnight in a refrigerator at 4°C for sufficient complexation. After the solution was degassed with nitrogen for 10 min, the initiator of N,N-dimethylaniline (5 μL) and benzoyl peroxide (0.0097 g) were added. The PS colloidal crystal template and glass substrates were held tightly together forming the "sandwich structure." The precursor solution was infiltrated into the PS colloid crystal template by capillary force until the colloidal crystal template became transparent. After polymerization at room temperature for 24 h, the resulting polymer composites

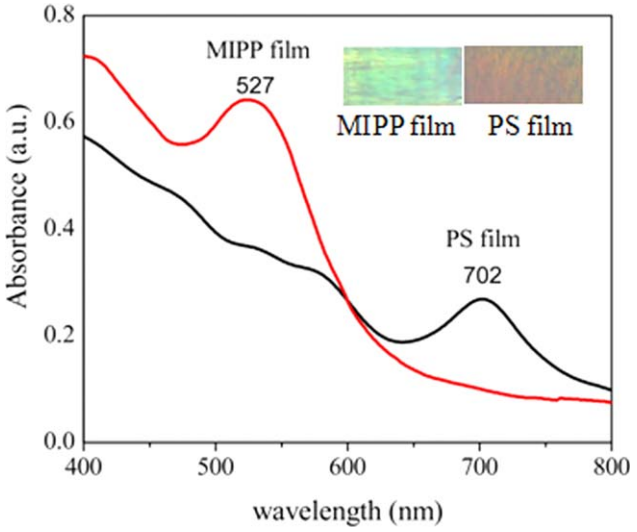

Figure 2. The absorption spectra of PS colloidal crystal film and MIPP film. [Color figure can be viewed in the online issue, which is available at wileyonlinelibrary.com.]

were immersed into tetrahydrofuran (THF) for 4 h to completely remove the PS template, then washed with methanol–acetic acid (9 : 1, v/v) solution to remove the cinchonine template, and finally was rinsed with anhydrous ethanol to obtain cinchonine MIPP film. The corresponding non-imprinted photonic polymer (NIPP) film was prepared in the same procedure without adding the cinchonine.

As a control experiment, the molecularly imprinted bulk polymer (MIBP) film was prepared with identical method as described for MIPP film, but without PS colloid crystal template. The corresponding non-imprinted bulk polymer (NIBP) was also prepared in the absence of both PS template and cinchonine imprinting template.

Binding Experiments

The polymer film (5 mg) were placed in a 10 mL conical flask and mixed with 2 mL of a known concentration of substrate solution in ethanol. The conical flask was oscillated at 30°C for 2 h. After the binding process was completed, the concentration of the free substrate in the solution was measured by a UV–vis spectrophotometer. The amount of substrate bound to the polymer (Q_e) was calculated by subtracting the amount of free substrate from the initial concentration.

Adsorption Kinetics

The polymer film (5 mg) was stuck tightly against the side of a quartz cell and mixed with 2 mL of 1.0 mmol/L cinchonine standard solution in ethanol. The absorbance was measured once every 30 seconds using the dynamic scanning procedure (UV–vis spectra testing software M. Wave Professional 1.1). The amount of cinchonine bound to the polymer (Q_t) at different time was calculated according to the absorbance.

Optical Measurement of MIPP Film

The solutions of cinchonine, quinine, and quinoline were prepared at concentration of 10^{-12}, 10^{-9}, 10^{-6}, and 10^{-3} mol/L in anhydrous ethanol, respectively. The MIPP was immersed into ethanol solution for 1 h to reach swollen equilibrium, and then dipped into the prepared substrate solutions one after another from low to high concentrations to eliminate interference. The Bragg diffraction wavelength shift was measured using a UV–vis spectrometer.

RESULTS AND DISCUSSION

Fabrication of Cinchonine MIPP Film

Colloidal template is commonly prepared by using the vertical deposition evaporation to make monodispersed colloidal particles into an ordered crystalline structure. In the present work, the synthesized monodispersed PS particles with a diameter of about 554 nm were used to form the colloidal template. The different concentrations of colloidal solution prepared with distilled water and ethanol in range of 5 mg/mL to 15 mg/mL were investigated at 45°C for 24 h, respectively. The result shows that the ordered close packed structure of colloidal crystal templates are easily obtained in the anhydrous ethanol. When the dispersion concentration of PS is optimized at 8 mg/mL, the prepared colloidal films are smooth and show little of fault and crack with a brilliant structural color.

The inverse opal structure of cinchonine MIPP was derived from the PS photonic crystal involving three steps. Firstly, the imprinting precursors were mixed and filled into the interstitial voids of PS colloidal crystal template. Then, the imprinting precursors were polymerized in the interspaces by triggering with a redox initiation system at room temperature. Finally, the PS template and cinchonine template were removed by the elution procedures. The pre-polymerization solution consisted in a mixture of template molecule cinchonine, functional monomer MAA, and cross-linker EDMA which favors hydrogen-bond and electrostatic interaction.[23] In order to make the polymerization at a relatively low temperature, which may prevent the solvent from volatilizing, the benzoyl peroxide and N,N-dimethylaniline as redox initiation system was utilized in this polymerization. After polymerization for 24 h, the resulting composites were washed with THF and methanol–acetic acid until complete removal of the opal template and the embedded cinchonine molecules from the imprinted polymer matrix. Figure 2 shows the adsorption spectra of PS colloidal crystal film and MIPP film. As shown in Figure 2, the obvious Bragg diffraction peaks of the PS colloidal crystal film and the inverse opal MIPP film

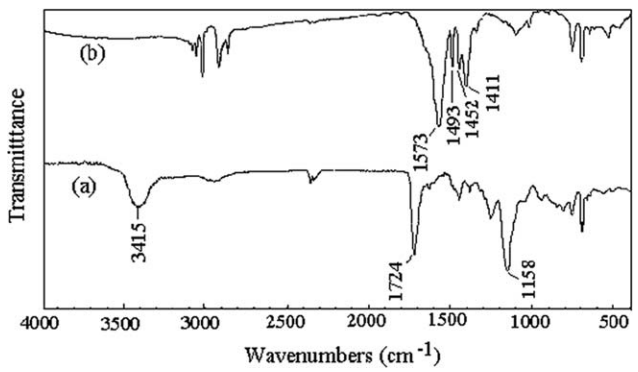

Figure 3. FT-IR spectra of prepared MIPP film (a) and the polystyrene (PS) colloidal crystal film (b).

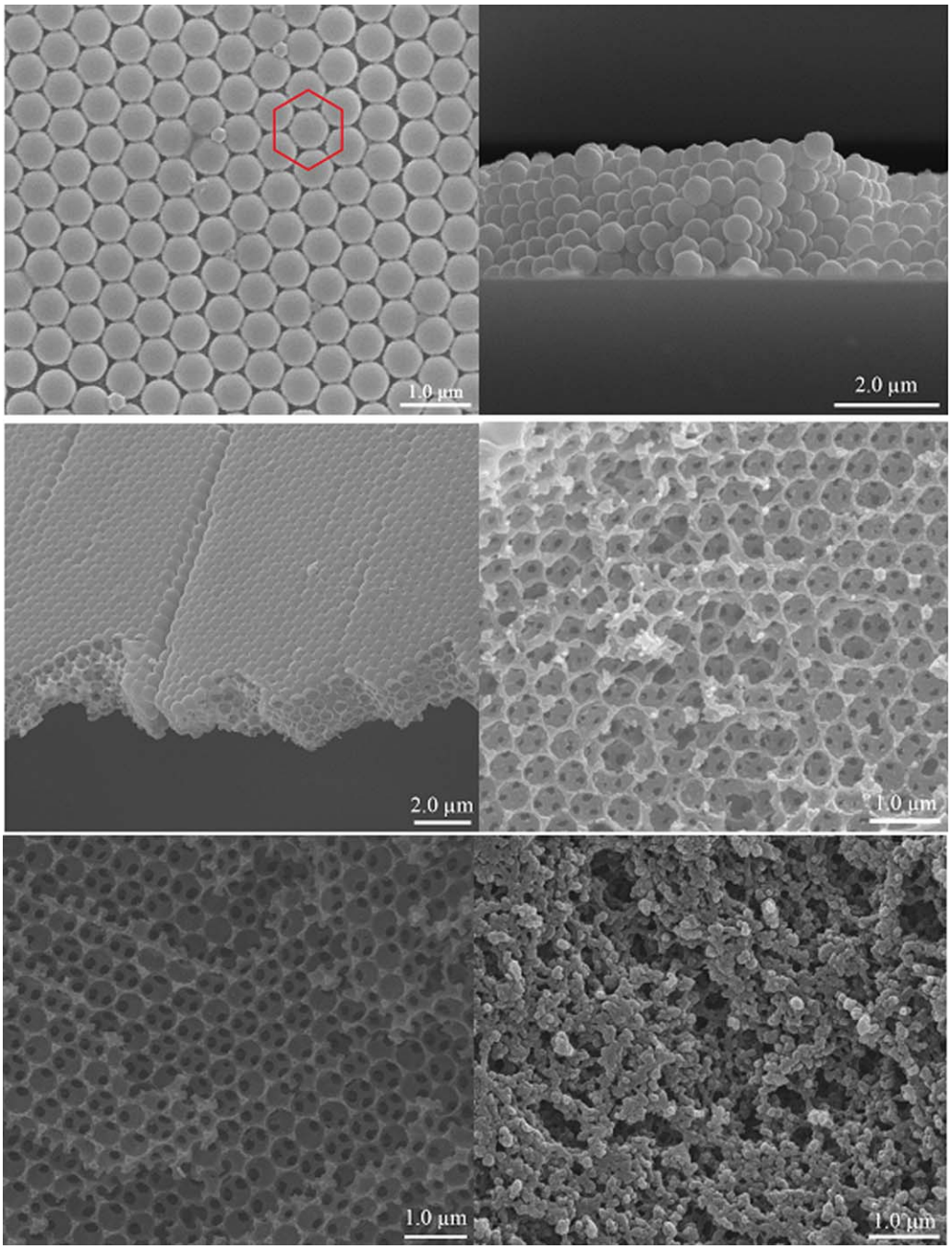

Figure 4. SEM images of PS colloidal crystal film of surface section (A) and cross-section (B), MIPP film of surface section (C) and inner section (D), NIPP film of inner section (E), and MIBP film of inner section (F). [Color figure can be viewed in the online issue, which is available at wileyonlinelibrary.com.]

appear at 702 nm and 527 nm, respectively, which indicate a highly 3DOM structure formed in the polymer films.

Characterization of MIPP

IR Spectra. Figure 3 shows the FT-IR spectra of the prepared MIPP film (a) and the PS film (b). In Figure 3, the strong peak at 3415 cm^{-1} and 1724 cm^{-1} in MIPP film are attributed to the stretching vibration of the hydroxyl group of MAA and carbonyl group of EDMA. Compared the IR spectrum of PS film with MIPP film, the characteristic bands of phenyl group at 1573 cm^{-1} and 1493 cm^{-1} disappear completely in the IR spectra of MIPP. These data suggest that the functional monomer and cross-linker had already been successfully polymerized in the initiation condition, and the polystyrene template and the cinchonine molecules were completely washed out from the imprinted film with THF and methanol–acetic acid, respectively.

Morphology Analysis. Figure 4 shows typical SEM images of the PS colloidal crystal film and the cinchonine MIPP film. It is clearly seen from Figure 4(A,B) that PS colloidal crystal film has

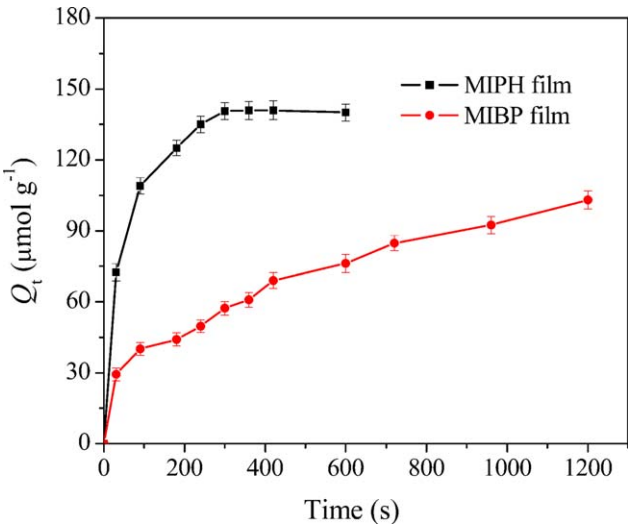

Figure 5. Curves of adsorption kinetics of MIPP and MIBP film. [Color figure can be viewed in the online issue, which is available at wileyonlinelibrary.com.]

a typical face-centered cubic (fcc) structure with (111) plane parallel to the substrate surface. The film assembles six layers with a thickness of about 3 μm. After removal of the PS template, the PS microspheres were converted to air spheres showing a hexagonal arrangement and surrounded by the imprinted polymer [Figure 4(C,D)]. The average macropore diameter is measured about 501 nm from SEM images, which represents about 9.6% shrinkage compared with the particle diameter (554 nm) of the PS micro-spheres template. However, for MIBP, the pores were formed from the liquid porogen. From the SEM image [Figure 4(F)], we can see that the structure of pores is obviously heterogeneous with a broad pore size distribution. The BET surface area of the MIPP and NIPP are about 21.86 m^2/g and 19.20 m^2/g, which is higher than that of the MIBP (13.83 m^2/g).

Binding Characteristics of MIPP Film

Figure 5 shows the adsorption kinetics of cinchonine solution onto MIPP film and traditional MIBP film. As seen from Figure 5, the binding amount Q_t (μmol/g) increases sharply with the increase of adsorption time, and the binding rate of cinchonine onto MIPP film was relatively faster than that onto MIBP film. The binding amount reached 86% of the maximum adsorption capacity in the first 3 min and the equilibrium was achieved within 5 min. However, for the MIBP film, it takes beyond 20 min to reach adsorption equilibrium. Therefore, in our case, it is easy for template molecules to reach the imprinting cavities of 3DOM MIPP and took less time to reach adsorption saturation. This may be attributed to the ordered macropores channels and the interconnecting porous structures in the polymer wall, which provide an excellent accessibility for imprinting molecule to recognition sites and improve the mass transport.

To get more insight into the binding characteristics of MIPP, a steady-state binding method and subsequent Scatchard analysis were carried out with the MIBP and their corresponding blank polymer as references. Their binding isotherms were determined in the initial concentration range of 0.2–2 mmol/L. The results of the binding experiments are shown in Figure 6. It can be seen that the binding amounts of the two kinds of polymer films increase with increasing the initial concentration of cinchonine, but the amounts of cinchonine binding to MIPP film are more than those of bulk MIBP one in the whole concentration range.

According to the obtained data of the adsorption study, the scatchard curve of polymers was obtained according to the equation[24]:

$$\frac{Q_e}{C_e} = \frac{Q_{\max} - Q_e}{K_d} \quad (1)$$

where Q_e (μmol/g) is the amount of cinchonine bound to the polymer, $Q_{\max}$ (μmol/g) is the maximum amount of cinchonine bound to the polymer, C_e (mmol/L) is the equilibrium concentration of cinchonine in the solution, and K_d (mmol/L) is the equilibrium dissociation constant.

The results show that the Scatchard plots of MIPP and MIBP can be fitted into two straight lines [Figure 7(A,B)], suggesting that the binding sites in the both polymers are heterogeneous and their affinities can be approximated by two dissociation constants (K_d) corresponding to high and low affinity sites, as usually observed for the MIPs via non-covalent molecular imprinting approach. However, for NIPP and NIBP [Figure 7(C,D)], the Scatchard plots are fitted only a single straight line due to the absence of the specific binding sites, and the adsorptions on them rely on the simplex non-specific interaction. The results agree with the work reported by Xu *et al.*,[25] where the MIP photonic films were prepared by using silica colloidal crystal template for creatinine. The fitted data are shown in Table I. The K_{d1} and K_{d2} are the high and the low affinity constant derived from the binding in low and high concentration of substrates, respectively. As seen in Table I, MIPP and MIBP present almost equal K_{d1} values, indicating that they have similarly

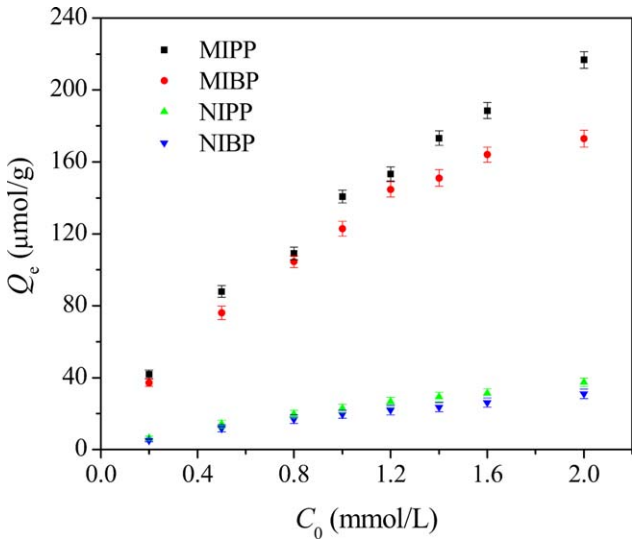

Figure 6. Adsorption isotherm of cinchonine onto MIPP and MIBP film. [Color figure can be viewed in the online issue, which is available at wileyonlinelibrary.com.]

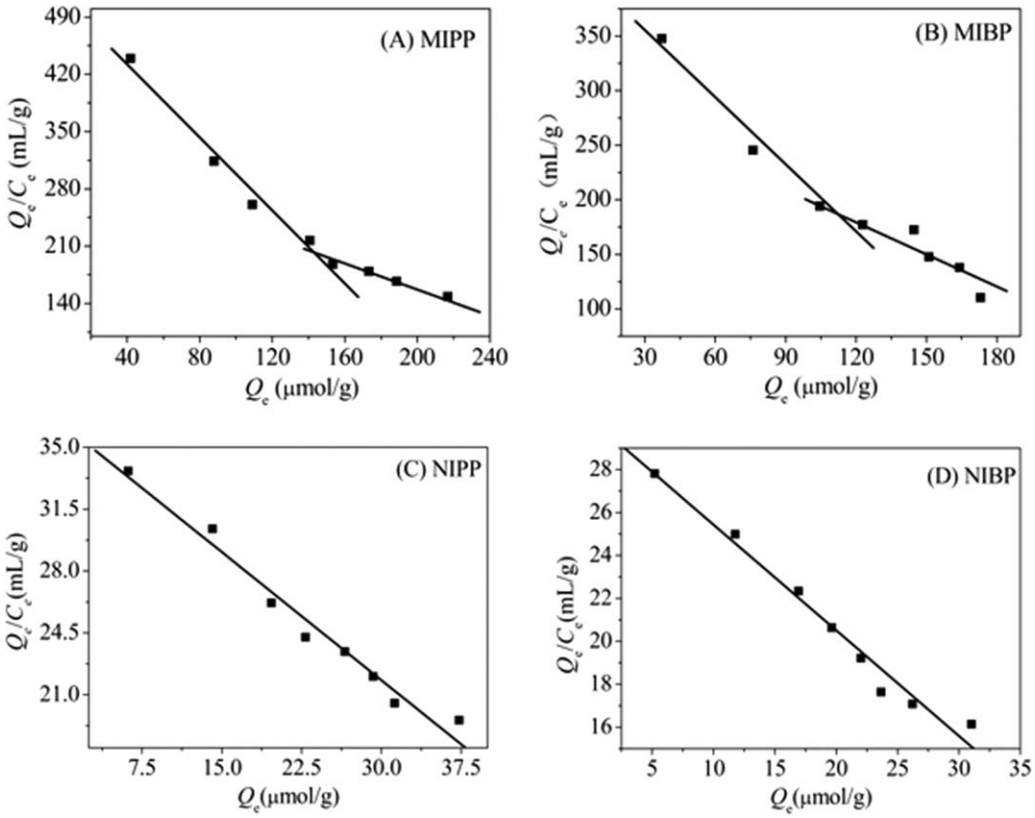

Figure 7. Scatchard plots to estimate the binding nature of the MIPP (A), MIBP (B), NIPP (C), and NIBP (D).

specific affinity ability to cinchonine. This can be attributed to the fact that both polymers were prepared using the same imprinting precursor recipe and formed the same recognition sites which were complementary to the template molecules on the functional group and the steric shape. However, the MIPP have higher Q_{max} values than those of MIBP. This phenomenon can be deduced that more efficient recognition sites were available in the MIPP film due to the high specific surface areas and easy accessibility for template molecules to the recognition sites through the porous structure.

Binding Specificity of MIPP Film

Comparison of the binding specificity of MIPP with MIBP films as well as their corresponding non-imprinted polymer films was performed by selecting cinchonine and its structural analogues, quinine and quinoline as the substrates. Their amounts of adsorption to polymers were determined with the equilibrium adsorption method. The specificity of MIPP was estimated by the distribution coefficients of the selected substrates between polymers and solution. The distribution coefficient K is defined according to the following equation[26]:

$$K = C_p / C_s \quad (2)$$

where C_p is the concentration of molecules on the polymers (μmol/g) and C_s is the concentration of molecules in the solution (mmol/L).

The distribution coefficients of the substrates are listed in Table II. As seen in Table II, the both imprinted films exhibit higher K values for cinchonine than their corresponding non-imprinted polymers. This demonstrates that the recognizing cavities based on stereo-shape and interaction sites have been created in resultant MIPP and MIBP polymers owing to the addition of template molecules during polymerization. Among the three selected substrates, the MIPP seems to prefer to bind cinchonine than the other two substrates. The K value of MIPP for cinchonine is the highest and reaches 148.44 mL/g, about

Table I. Isotherm Fitting Data for the Adsorption of Cinchonine by MIPP/NIPP and MIBP/NIBP

Polymers	K_{d1} (mmol/L)	Q_{max1} (μmol/g)	K_{d2} (mmol/L)	Q_{max2} (μmol/g)
MIPP	0.45	234.81	1.59	453.55
NIPP	-	-	2.08	75.65
MIBP	0.49	199.58	1.03	314.35
NIBP	-	-	2.04	61.94

Table II. The K Value of Substrates on MIPP/NIPP and MIBP/NIBP Film[a]

Substrate	MIPP	NIPP	MIBP	NIBP
Cinchonine	148.44	19.65	66.17	16.12
Quinine	39.69	15.82	31.25	14.98
Quinoline	30.05	7.35	26.13	3.94

[a] Initial concentration of substrates: 2.0 mmol/L; volume: 2 mL; solvent: ethanol; and binding time: 2 h.

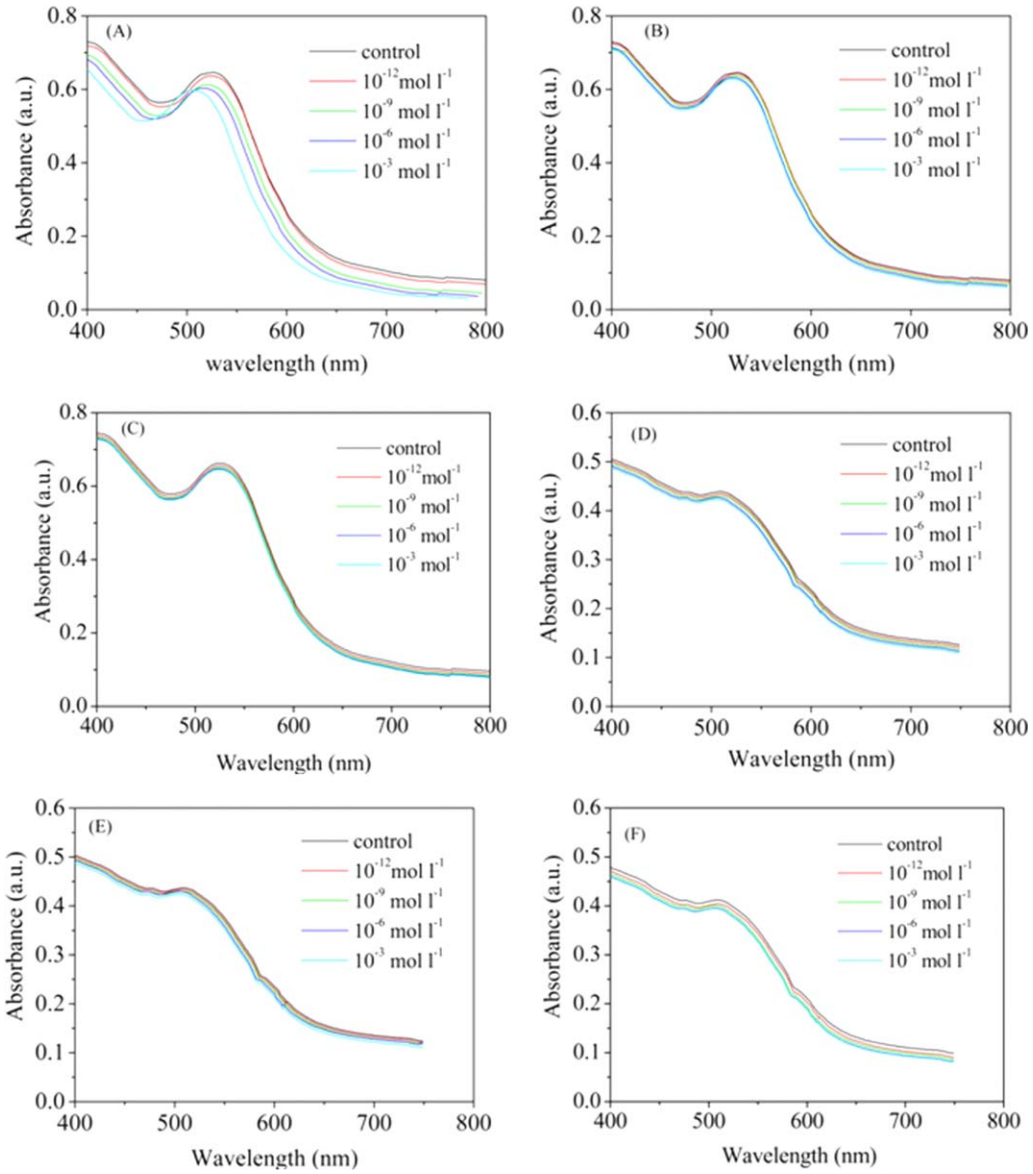

Figure 8. Optical response of the MIPP to different concentrations of cinchonine (A), quinine (B), and quinoline (C); optical response of the NIPP to different concentrations of cinchonine (D), quinine (E), and quinoline (F). [Color figure can be viewed in the online issue, which is available at wileyonlinelibrary.com.]

2.2 times higher than that of MIBP for cinchonine. However, both NIPP and NIBP show relatively low *K* values for all tested substrates. These results indicate that the improved binding selectivity is obtained for the MIPP film via colloidal crystal template technique in our case.

Optical Responsive Properties of MIPP Film

To investigate the optical responsive properties and its sensing specificity of the MIPP, the inverse opal MIPP film were soaked in a series of concentrations of cinchonine, quinine, and quinoline solution, respectively. Figure 8(A,B) shows the results of Bragg diffraction shift and optical response of MIPP. As shown in Figure 8(A), the Bragg diffraction peak of MIPP shows a gradual blue shift with increasing the concentration of cinchonine. The maximum adsorption wavelength changes from 527 to 503 nm with increasing the concentration of cinchonine from 0 to 10^{-3} mol/L. However, in quinine and quinoline solution, the Bragg diffractive peak remained nearly constant with increasing the concentration of quinine [Figure 8(B,C)]. The results clearly indicate that the MIPP has highly specific and sensitive response to the template molecules. This may be caused by the changes of microenvironments created by the molecular imprinting process. Owing to the recognition specificity of MIPP, the cinchonine can specifically bind the imprinted nanocavities within the MIPP film. When the imprinted cavities are occupied by cinchonine molecules instead of ethanol solvent, the lattice constants and the average refractive indices of the photonic polymer will be changed. These changes induce the shift of the Bragg diffraction.

In the control, NIPP was also soaked in cinchonine, quinine, and quinoline solution, respectively. As shown in Figure 8(D–

Table III. Reproducibility of MIPP about its Binding Capacity and Optical Responsive Properties[a]

Repeated parameters	1	2	3	4	5
Q/μmol/g	216.72	215.12	213.35	211.75	210.90
λ_0/nm	527	527	526	525	524
λ_c/nm	503	503	502	502	501

[a] Q, the binding amount measured in 2 mmol/L of cinchonine solution; λ_0, the Bragg diffraction wavelength of MIPP in the ethanol solvent without template molecules; λ_c, the Bragg diffraction wavelength of MIPP soaking in 10^{-3} mol/L of cinchonine solution.

F), it was interesting to note that no obvious changes in the Bragg peak shifts of NIPP are observed compared with that of MIPP at the same concentration of substrates, probably due to no specific binding sites in the NIPP for the three substrates. The results suggest that special recognition is mainly responsible for the optical responsive behaviors of MIPP.

Reproducibility of MIPP Film

The reproducibility of 3DOM MIPP film about its binding ability and optical responsive properties were investigated using five cycles. After adsorption, the MIPP was eluted using methanol–acetic acid (9:1, v/v) to remove the binding analytes and followed by rinsing with anhydrous ethanol to restore the original status. Subsequently, the MIPP was then immersed into cinchonine solution for rebinding and its binding amount and Bragg diffraction were measured. Thus, five cycles of adsorption, elution, and rebinding/optical measuring were performed in different concentration of cinchonine solution. The results (Table III) indicate that the MIPP film are very stable and its binding capacity only decreased by about 2.69%, and the optical Bragg diffraction peak also shows only slight wavelength fluctuation, which reflect the reusability and recoverability of the imprinted film in the binding ability and optical responsiveness.

CONCLUSIONS

In this article, we have developed a new approach for preparing MIPP with highly 3DOM array based on the combination of PS photonic crystal template method and molecular imprinting techniques. The imprinted film shows great advantages of having a rapid adsorption kinetics, improved binding capacity, and specificity to template molecules. The recognition events of MIPP could be directly transferred into readable optical signals through a change in Bragg diffraction, suggesting good application prospects as sensor elements for rapid on-site detection of chemo/biomolecules.

ACKNOWLEDGMENTS

This work was financially supported by the National Natural Science Foundation of China (No, 81303199), Distinguished Young Talents in Higher Education of Guangdong, China (No, K5090006) and the Special Funds from Central Finance of China in Support of the Development of Local Colleges and University [Educational finance Grant No.276 (2014)].

REFERENCES

1. Baggiani, C.; Baravalle, P.; Giraudi, G.; Tozzi, C. *J. Chromatogr. A* **2007**, *1141*, 158.
2. Cheng, W. J.; Ma, H. T.; Zhang, L.; Wang, Y. *Talanta* **2014**, *120*, 255.
3. Sun, H.; Lai, J. P.; Fung, Y. S. *J. Chromatogr. A* **2014**, *1358*, 303.
4. Tan, J.; Jiang, Z. T.; Li, R.; Yan, X. P. *Trends Anal. Chem.* **2012**, *39*, 207.
5. Cirillo, G.; Curcio, M.; Parisi, O. I.; Puoci, F.; Lemma, F.; Spizzirri, U. G.; Picci, N. *Pharm. Dev. Technol.* **2010**, *15*, 526.
6. Huang, C. Y.; Syu, M. J.; Chang, Y. S.; Chang, C. H.; Chou, T. C.; Liu, B. D. *Biosens. Bioelectron.* **2007**, *22*, 1694.
7. Urraca, J. L.; Moreno-Bondi, M. C.; Orellana, G.; Sellergren, B.; Hall, A. *Anal. Chem.* **2007**, *79*, 4915.
8. Saylan, Y.; Üzek, R.; Uzun, L.; Denizli, A. *J. Biomater. Sci. Polym. Ed.* **2014**, *25*, 881.
9. Guan, G. J.; Liu, B. H.; Wang, Z. Y.; Zhang, Z. P. *Sensors* **2008**, *8*, 8291.
10. Xu, S. F.; Chen, L. X.; Li, J. H.; Wei, Q.; Ma, J. P. *J. Mater. Chem.* **2011**, *21*, 12047.
11. Xuan, J.; Jiang, L. P.; Zhu, J. J. *Chin. J. Anal. Chem.* **2010**, *38*, 513.
12. Yang, L. Y.; Liau, W. B. *Synth. Met.* **2010**, *160*, 1809.
13. Xia, Y.; Gates, B.; Yin, Y.; Liu, Y. *Adv. Mater.* **2000**, *12*, 693.
14. Li, J. H.; Zhang, Z.; Xu, S. F.; Chen, L. Q.; Zhou, N.; Xiong, H.; Peng, H. L. *J. Mater. Chem.* **2011**, *21*, 19267.
15. Wang, L. Q.; Lin, F. Y.; Yu, L. P. *Analyst* **2012**, *137*, 3502.
16. Zhou, C. H.; Wang, T. T.; Li, J. Q.; Guo, C.; Peng, Y.; Bai, J. L.; Liu, M.; Dong, J. W.; Gao, N.; Ning, B. A.; Gao, Z. X. *Analyst* **2012**, *137*, 4469.
17. Liu, F.; Huang, S. Y.; Xue, F.; Wang, Y. F.; Meng, Z. H.; Xue, M. *Biosens. Bioelectron.* **2012**, *32*, 273.
18. Xu, D.; Zhu, W.; Wang, C.; Tian, T.; Li, J.; Lan, Y.; Zhang, G. X.; Zhang, D. Q.; Li, G. T. *Chem. Commun.* **2014**, *50*, 14133.
19. Wu, Y. N.; Li, F. T.; Xu, Y. X.; Zhu, W.; Tao, C. A.; Cui, J. C.; Li, G. T. *Chem. Commun.* **2011**, *36*, 10094.
20. Xu, D.; Zhu, W.; An, Q.; Li, W. N.; Li, X. S.; Yang, H. W.; Yin, J. X.; Li, G. T. *Chem. Commun.* **2012**, *48*, 3494.
21. Matsui, J.; Nicholls, I. A.; Takeuchi, T. *Tetrahedron: Asymmetry* **1996**, *7*, 1357.
22. Holland, B. T.; Blanford, C. F.; Do, T.; Stein, A. *Chem. Mater.* **1999**, *11*, 795.
23. He, J. F.; Zhu, Q. H.; Deng, Q. Y. *Spectrochim. Acta A* **2007**, *67*, 1297.
24. Zhou, J.; He, X. W. *Anal. Chim. Acta* **1999**, *394*, 353.
25. Xu, D.; Zhu, W.; Jiang, Y.; Li, X. S.; Li, W. N.; Cui, J. C. Y. J. X.; Li, G. T. *J. Mater. Chem.* **2012**, *22*, 16572.
26. Xu, Z. F.; Liu, L.; Deng, Q. Y. *J. Pharm. Biomed. Anal.* **2006**, *41*, 701.